

# Soft Matter

Accepted Manuscript



This is an *Accepted Manuscript*, which has been through the Royal Society of Chemistry peer review process and has been accepted for publication.

*Accepted Manuscripts* are published online shortly after acceptance, before technical editing, formatting and proof reading. Using this free service, authors can make their results available to the community, in citable form, before we publish the edited article. We will replace this *Accepted Manuscript* with the edited and formatted *Advance Article* as soon as it is available.

You can find more information about *Accepted Manuscripts* in the [Information for Authors](#).

Please note that technical editing may introduce minor changes to the text and/or graphics, which may alter content. The journal's standard [Terms & Conditions](#) and the [Ethical guidelines](#) still apply. In no event shall the Royal Society of Chemistry be held responsible for any errors or omissions in this *Accepted Manuscript* or any consequences arising from the use of any information it contains.



Journal Name

ARTICLE

## Phase behaviour of the ternary system: Monoolein/Water/branched Polyethylenimine

Manoj Kumar, Guruswamy Kumaraswamy

Received 00th January 20xx,  
Accepted 00th January 20xx

DOI: 10.1039/x0xx00000x

www.rsc.org/

Addition of a branched polymer, polyethylene imine, significantly alters the organization of a glycerol monooleate (GMO) lipid/water system. We present detailed data over a wide range of composition (water content from 10-40%, relative to GMO; PEI fractions from 0-4%) and temperature (25-80°C). PEI molecular weight effects are examined using polymers over a range from 0.8 to 25 kDa. Addition of PEI induces the formation of higher curvature reverse phases. In particular, PEI induces the formation of the Fd3m phase: a discontinuous phase comprising reverse micelles of two different sizes stacked in a cubic AB<sub>2</sub> crystal. Formation of the Fd3m phase at room temperature, on addition of polar, water soluble PEI is unusual, since, such phases typically form only on addition of apolar oils. The largest stability window for the Fd3m phase is observed for PEI of molecular weight = 2kDa. We discuss how PEI influences the formation and stability of high curvature phases.

### Introduction:

Organized lipid/water systems are important since they are encountered in several biological processes<sup>1</sup> and, since they have wide ranging technological applications.<sup>2-7</sup> Specifically, glycerol monooleate (or GMO) has emerged as molecule with great promise as a nanostructured amphiphilic delivery vehicle.<sup>8-11</sup> GMO is a hydrophobic lipid (HLB value = 3.8) that is commercially used as a food emulsifier. The GMO/water system exhibits rich phase behaviour at room temperature, forming lamellar and, bicontinuous cubic phases with gyroid and double diamond architectures. Due to the large miscibility gap for the lipid, the double diamond bicontinuous phase can coexist with excess water.<sup>12</sup> This allows formulation of the extremely rigid and hard-to-process cubic phases into low viscosity aqueous dispersions of lipid particles with internal mesophase structure.<sup>13-14</sup> Recently, novel processing strategies have emerged to prepare nanostructured oil-in-water and water-in-oil emulsions that have significant application potential.<sup>15</sup>

Useful functional materials can be realized by introduction of colloidal nanoparticles or polymers within mesophases.<sup>16</sup> Incorporation of polymers in a mesophase is governed by a complex interplay of polymer-mesophase interactions and, the conformational entropy change of the polymer on

confinement in the mesophase.<sup>17-20</sup> Incorporation of ternary components can also result in a change in mesophase organization.<sup>21-31</sup> Typically, the effect of addition of a ternary component is rationalized through its effect on the packing parameter,  $P = v/Al$ ,<sup>32</sup> (where  $v$  and  $l$  are the volume and length of the hydrophobic tail, and  $A$  is the area of the polar head group). The packing parameter presents a convenient geometric framework to interpret mesophase behaviour. For  $P = 1$ , the lamellar phase forms. For  $P \approx 1/2$ , the increase in effective head group size is accommodated by increasing the curvature of the self-assembled lipid structure and, a hexagonal phase forms. For  $P \approx 1/3$ , higher curvature micellar phases are observed. Similarly, an increase in  $P$  results in formation of mesophases with reverse curvature (viz. reverse water in oil phases). Incorporation of ternary components influences  $P$  and, therefore changes the curvature. Thus, for example, incorporation of phosphatidylinositol promotes membrane curvature in model dioleoylphosphatidylcholine membranes.<sup>33</sup>

In GMO/water systems, Caffrey has demonstrated that addition of alkyl glycosides results in a decrease in  $P$  towards 1, such that bicontinuous cubic phases transform into lamellar phases.<sup>34</sup> On the other hand, addition of sugars is reported to result in a decrease the lattice parameter in GMO/water, favouring the formation of high curvature inverse phases.<sup>21,35-36</sup> While formation of the reverse hexagonal phase has been reported on addition of several ternary hydrophilic moieties,<sup>37</sup> the ordered reverse micellar Fd3m phase typically forms only on addition of apolar oils. These apolar oils are localized in the spaces around the reverse micelles and solubilize the lipid tails. Thus, hydrophobic lipids like monolinolein (MLO) and, monoolein (GMO) readily form the Fd3m phase on addition of oils such as tetradecane(TC)<sup>38-39</sup> or limolene,<sup>40</sup> hexadecane<sup>41</sup>

Complex Fluids and Polymer Engineering Group, Polymer Science and Engineering Division, CSIR-National Chemical Laboratory, Dr. Homi Bhabha Road, Pune 411008, Maharashtra, India. Phone: +91-20-2590-2182; Email: g.kumaraswamy@ncl.res.in.

† Footnotes relating to the title and/or authors should appear here. Electronic Supplementary Information (ESI) available: [details of any supplementary information available should be included here]. See DOI: 10.1039/x0xx00000x

(HD) or Vitamin-E.<sup>42</sup> The Fd3m phase is also observed to form in phospholipids on addition of apolar components.<sup>43,44</sup> In these examples, formation of the Fd3m phase results since the apolar oils relieve the packing frustration of lipid tails.<sup>45-47</sup>

Recently, we reported that addition of a small quantity of hydrophilic polymer could result in transformation of the GMO/water system into an Fd3m phase, without any added oil.<sup>48</sup> We demonstrated that polar macromolecular entities (i) with a compact architecture and, (ii) bearing groups that interacted strongly with the GMO headgroup, were capable of inducing sufficient curvature in the lipid assembly to form an Fd3m phase. Thus, polyamidoamine (PAMAM) dendrons with terminal amine groups that interact with the GMO, and with a compact dendritic structure induced the Fd3m phase in GMO/water while, remarkably, the linear analogue of the PAMAM did not. Thus, we established a new route to tuning the curvature of GMO/water assemblies that is critically dependent on the chain architecture of the ternary polar polymeric inclusion. Synthesis of perfectly branched PAMAM dendrons is challenging. However, we have established that other readily available polar ternary inclusions, such as branched polyethylenimine and silsesquioxane cages that have compact molecular shapes and that interact strongly with GMO also induce the formation of the Fd3m phase.

In this work, we explore the GMO/water/branched PEI phase diagram in detail. Polyethylenimine (PEI) interacts strongly with phospholipid bilayers<sup>49</sup> and has been reported to be a highly effective non-viral vector for gene delivery to cells. PEI is a branched polymer that bears primary, secondary and tertiary amine groups. As the PEI amine groups are protonated at different pH,<sup>50</sup> we can use variable pH NMR studies to probe the structure of branched PEI. The structure of the PEI used in this work was characterized previously.<sup>51</sup> In this work, we examine systems whose pH is maintained at 10, where the PEI amines have a very low degree of protonation. Operating at a pH = 10 also ensures that the GMO does not undergo hydrolytic degradation. We present a comprehensive study of the equilibrium phase behaviour that explores the effect of addition of small weight fractions of PEI (up to 4% by weight) to GMO/water. We examine various GMO/water ratios (weight fractions of water ranging from 10-40%) at temperatures from ambient (25°C) to 80°C. We also explore the effect of PEI molecular weight by investigating polymers with molecular weights of 0.8, 2 and 25 kDa. This work demonstrates the composition window in which the GMO/water/PEI system forms the Fd3m phase and establishes that there is an optimal PEI molecular weight at which the Fd3m is most stable.

## Experimental:

### Materials and methods:

Glycerol monooleate (trade name: Rylo MG 20 Pharma, Schematic in Figure 1) was generously supplied by Danisco India. In this work, we refer to the commercial Rylo Sample as GMO. Glycerol monooleate (GMO) is a non-ionic lipid molecule with an HLB value

of 3.8.<sup>8</sup> We have performed acid-base titration on Rylo and measure an acid value of 2.3.

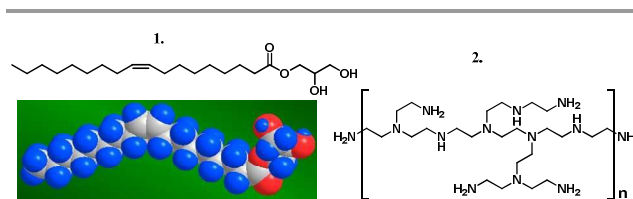


**Figure 1:** (1a) Structure of GMO; (1b) 3D configuration of GMO; (2) A schematic representation of branched PEI containing primary, secondary and tertiary amines.

We have previously reported detailed characterisation of GMO.<sup>11</sup> All experiments were carried out with the same batch of GMO that was stored at -80°C to avoid degradation. Polyethylenimine (PEI) of different molecular weight (Supplier specified as  $M_w = 0.8$  kDa, PDI = 1.3; 2 kDa, PDI = 1.1 and 25 kDa, PDI = 2.5), and with a branched architecture, were obtained as aqueous dispersions from Sigma Aldrich and used as received (Schematic in Figure 1). High purity glycerol monooleate (HP-GMO, purity > 99.9%) was purchased from Sigma Aldrich and used as received.

GMO/water/PEI ternary samples were prepared at constant pH (= 10, by decreasing the pH using 70% w/v nitric acid solution, obtained from Merck India). All samples were prepared using distilled deionised water of resistivity 18.2 MΩ.cm. The nomenclature followed in this work is:  $f_w$  represents the weight fraction of water relative to GMO while,  $\Phi$  represents the weight fraction of added PEI in the GMO/water/PEI system. Thus, for example, a system with  $f_w = 20\%$  and  $\Phi = 2\%$  comprises (by weight) 78.4% GMO, 19.6% water ( $78.4 + 19.6 = 98$ ;  $19.6 / (78.4 + 19.6) = 0.2$ ) and 2% PEI. In a typical sample preparation, we first thaw the GMO in an oven at ~80°C. We use a 50 wt% aqueous PEI stock solution (pH = 12.8) and directly add this to GMO. Water is added to adjust the ratio of GMO to water and, to adjust the pH to 10. For example, 1 g of a sample containing 90:10 GMO:water, with 2% PEI was prepared by adding 4 mg of the PEI stock solution (50 wt%) to 78 mg of water, and then adding this to 882 mg of GMO warmed to 80°C. GMO, water and PEI were mixed in a closed vial and the temperature was repeatedly cycled to 80°C. Finally, the sample was equilibrated in the vial by storing for 10 to 15 days at room temperature. Other GMO/water/PEI compositions were prepared in a similar manner.

We measured pH using a Mettler Toledo instrument (SevenMulti), calibrated with standard pH solutions. Samples were characterized using Small-angle X-ray scattering (SAXS) and, polarised optical microscopy (POM). SAXS was performed using a Bruker Nanostar equipped with Cu rotating anode, tungsten filament, and three pinhole collimation. We operated the SAXS at a voltage of 45kV and 18mA current. Data was collected using a 2D gas filled HiStar detector, over a q-range

of 0.01–0.2  $\text{\AA}^{-1}$  (sample to detector distance of 105 cm). The detector was calibrated using a standard silver behenate sample. Data was collected until the detector registered at least a million counts. The scattered 2-D data is isotropic and is circularly averaged using Bruker offline software to reduce to 1-D. Samples were filled in a capillary tube (diameter 2 mm; wall thickness  $\sim 10 \mu\text{m}$ ) with a metal holder. Samples loaded in the capillaries were heated to 90°C to eliminate the effect of shearing while loading in the capillary and then cooled to room temperature for measurements. Temperature dependent experiments were performed using a Peltier heating stage. The temperature was controlled using an MCU temperature controller, to an accuracy of  $\pm 0.1^\circ\text{C}$ .

Optical microscopy was performed on an Olympus BX-50, mounted with a Nikon camera. We used a CSS450 Linkam stage for controlled heating of the samples. Samples were sandwiched between the heated bottom plate of the CSS450 and a glass cover slip. Samples were heated at 5°C/minute to 80°C and subsequently cooled to room temperature.

## Results and Discussions:

We begin with a description of ternary systems containing PEI with a molecular weight of 2 kDa in GMO/water. We describe the equilibrium phases formed by this ternary system at room temperature for  $10\% \leq f_w \leq 40\%$  and for  $\Phi \leq 4\%$ . Subsequently, we examine the temperature dependence of the phase behaviour and, present the phase diagram in composition-temperature space. Finally, we investigate the effect of varying the molecular weight of the PEI.

### a. GMO/water/PEI-2kDa organization at room temperature: Variation of PEI concentration ( $\Phi$ ) and water content ( $f_w$ ):

An 85/15 GMO/water binary system (viz.  $f_w = 15\%$ ,  $\Phi = 0$ ) forms a lamellar ( $L_\alpha$ ) phase at room temperature ( $= 25^\circ\text{C}$ ) (Figure 2). The lamellar phase is identified by characteristic

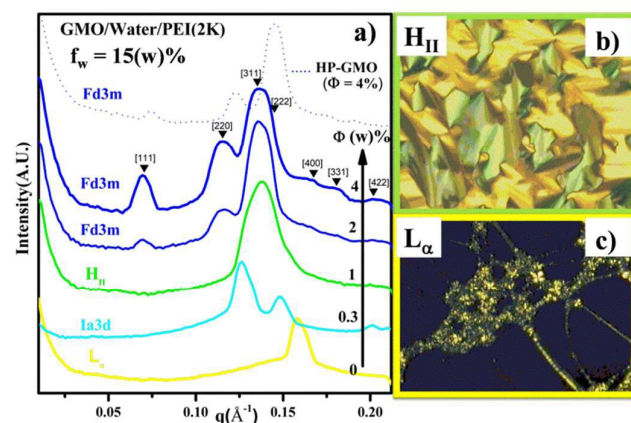


**Figure 2:** (a) SAXS for GMO/water/2kDa PEI systems ( $f_w = 15\%$ ) as a function of PEI fraction ( $\Phi$ ). Data for ternary systems containing HP-GMO is also shown. Optical micrograph between crossed polarizers for the ternary system at (b)  $\Phi = 0\%$  ( $L_\alpha$  phase) and (c)  $\Phi = 1\%$  ( $H_{II}$  phase).

streak-shaped textures between crossed polarizers (Figure 2 c). SAXS on lamellar phases gives peaks whose positions are in the ratio of 1:2:3:.. We observe a SAXS peak at  $q = 0.160 \text{\AA}^{-1}$ , corresponding to a d-spacing of 39 Å (Figure 2). Higher order peaks cannot be observed as the SAXS instrument configuration limits the  $q$  range to less than  $0.2 \text{\AA}^{-1}$ .

On addition of a small fraction of PEI ( $\Phi = 0.3\%$ ), the  $L_\alpha$  phase transforms into a bicontinuous cubic Ia3d phase. This phase is characterized by SAXS peaks, whose peak positions are in the ratio of  $\sqrt{6} : \sqrt{8} : \sqrt{14}$  (Figure 2 a). For higher PEI concentrations ( $\Phi = 1\%$ ) the system organizes into an inverse hexagonal phase ( $H_{II}$ ), that is characterized by cone type textures between crossed polarizers (Figure 2 b). SAXS peak positions from the  $H_{II}$  phase are in the ratio of 1:  $\sqrt{3}$ :  $\sqrt{4}$ :  $\sqrt{7}$ ... Again, as for the  $L_\alpha$  phase, only the first SAXS peak is observed in the experimental  $q$ -range, and this corresponds to a d-spacing of 46 Å. On further increasing  $\Phi$  to 2%, the  $H_{II}$  phase transforms into a discontinuous phase with Fd3m symmetry, identified using the SAXS peak positions.

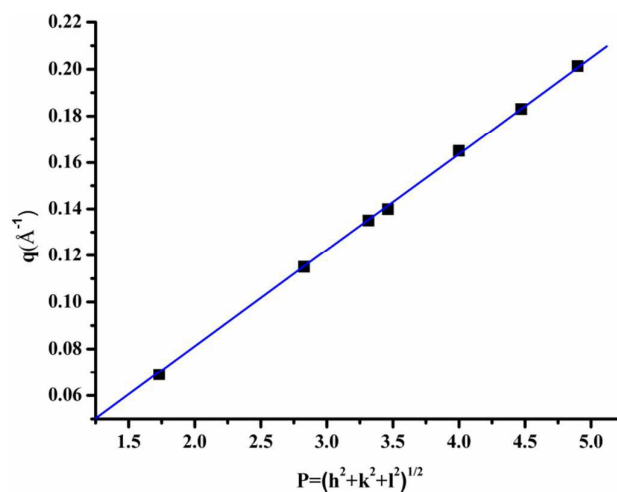


**Figure 3:** A plot of the peak reciprocal spacing,  $q (\text{\AA}^{-1})$  as a function of  $P = (h^2 + k^2 + l^2)^{1/2}$  is a straight line through the origin.

We identify 7 peaks for the Fd3m phase, and index these in accordance to literature reports.<sup>2,52</sup> A plot of the peak positions against  $(h^2 + k^2 + l^2)^{1/2}$ , where  $h, k, l$  are the Miller indices that characterize the peak, is a straight line passing through the origin (Figure 3). This confirms that the GMO/water/2kDa PEI system forms an Fd3m phase for  $f_w = 15\%$  and  $\Phi = 2\%$ . From the SAXS data, we calculate the lattice parameter associated with the Fd3m phase as 157 Å. The Fd3m phase comprises reverse micelles of two different sizes organized into cubic order to form an  $AB_2$  crystal structure. Due to the cubic symmetry of the Fd3m phase, it appears dark between crossed polarizers. We observe that the formation of the Fd3m phase is correlated with the development of turbidity.

Previously, discontinuous reverse micellar Fd3m phases have been reported to form in lipid systems only on addition of apolar ternary components.<sup>38–42</sup> Therefore, the formation of



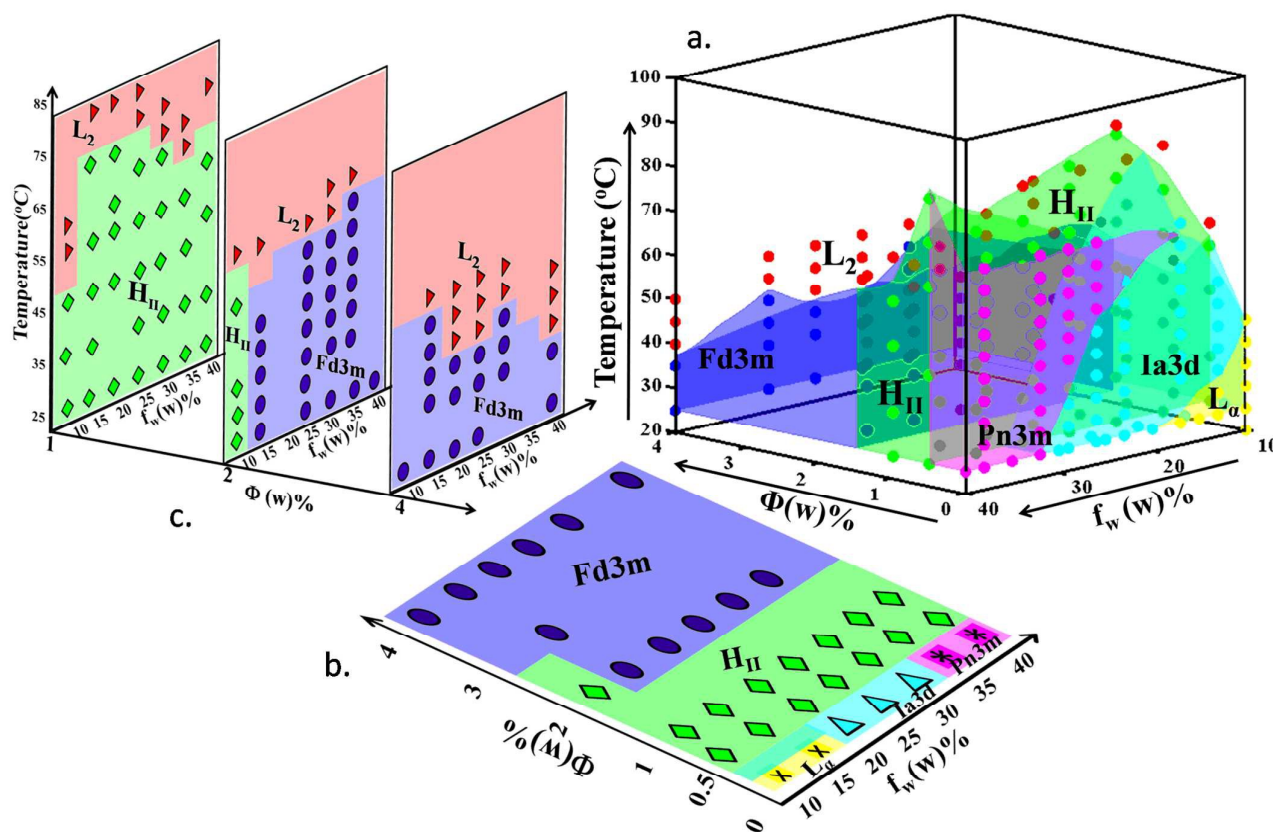


**Figure 4:** (a) Ternary GMO/H<sub>2</sub>O/2kDa PEI phase diagram as a function of  $f_w$ ,  $\Phi$  and temperature. Slices of the phase diagram showing the phase behaviour at (b)  $T = 25^\circ\text{C}$ ; (c)  $\Phi = 1, 2$  and  $4\%$

an  $Fd3m$  phase on addition of water soluble, polar PEI must follow a different path. Addition of hydrophilic molecules, such as glucose, has been reported<sup>21</sup> to shift the  $L_\alpha$ /cubic/ $H_{II}$  phase boundaries in lipid-water systems, in a manner similar<sup>32</sup> to this work. This has been rationalized by considering the packing parameter,  $P$ , defined earlier. Addition of hydrophilic molecules reduces hydration of the head group, thus shrinking  $A$ . This results in an increase in  $P$ , and a tendency to transform from the lamellar phase to cubic and then to hexagonal. Formation of a reverse micellar phase on addition of hydrophilic moieties would necessitate an increase in  $P$  from 1 (that characterizes the  $L_\alpha$  phase). Geometric rules for the critical packing parameter that govern formation of reverse phases have not been reported. However, if we assume that the critical packing parameter for reverse micellar phase formation is  $P = (1/3)^{-1} = 3$ , then this corresponds to a nearly 3-fold reduction in  $A$ . We believe that such a large reduction in

the effective  $A$ , by dehydration of the head group by PEI is unlikely. Therefore, for the GMO/water/PEI systems, the mechanistic origin of the phase transition cannot be attributed to geometric packing considerations.

Recently, we have demonstrated<sup>48</sup> that while compact dendritic ternary additives induce the formation of the  $Fd3m$  phase in GMO/water, their linear analogues do not. This is consistent with our hypothesis that geometric packing considerations alone cannot explain these transitions. Rather, we believe that the formation of the  $Fd3m$  phase arises from a strong attractive interaction between the GMO head group and the compact, branched PEI molecules. This is consistent with the data presented here on GMO/water/PEI systems. It is remarkable that only very small added fractions of the PEI are sufficient to induce phase transitions in the GMO/water system: the  $H_{II}$  phase forms on addition of only  $\Phi = 1\%$  PEI, while the  $Fd3m$  phase forms on addition of as little as  $\Phi = 2\%$

PEI. In comparison, we note that in GMO/water/oil ternary systems,  $\approx 20\%$  of apolar oil needs to be added to form the Fd3m phase.

The Fd3m phase persists on increasing the PEI content to  $\Phi = 4\%$  (Figure 2). We note that the d spacing that characterizes the Fd3m phase does not change significantly on increasing  $\Phi$  from 2% (156 Å) to 4% (157 Å). Formation of the Fd3m phase in the GMO/water/PEI ternary system cannot be attributed to impurities in the commercial GMO used in this investigation. We have prepared a few ternary compositions containing high purity GMO (HP-GMO), water and 2kDa PEI, and observe qualitatively similar phase behaviour. For example, the ternary system prepared using HP-GMO at  $f_w = 15\%$ ,  $\Phi = 4\%$  also shows the formation of the Fd3m phase (Figure 2a, dotted line). However, we observe that there is a decrease in the d-spacing for the Fd3m phase prepared using HP-GMO (to 78.5 Å, relative to 91 Å for commercial GMO).

We observe that at all  $f_w$  between 10-40%, the GMO/water system transitions to the  $H_{II}$  phase, and subsequently to the Fd3m phase with increase in PEI content,  $\Phi$  (Figure 4). For  $f_w = 10\%$ , increasing  $\Phi$  results in transformation of the  $L_\alpha$  phase into a bicontinuous Ia3d phase (at low  $\Phi = 0.3\%$ ),  $H_{II}$  phase (for  $\Phi \leq 2\%$ ) and formation of a discontinuous reverse micellar Fd3m phase for  $\Phi = 4\%$ . Thus, while the sequence of phase transitions with increasing  $\Phi$  ( $L_\alpha$  to Ia3d to  $H_{II}$  to Fd3m) is similar for  $f_w = 10$  and 15%, the window for  $H_{II}$  phase formation ( $\Phi \leq 2\%$ ) is larger for  $f_w = 10\%$ .

With increase in water content,  $20\% \leq f_w \leq 30\%$ , the binary GMO/water system forms the Ia3d phase. The Ia3d phase is retained for addition of small fractions of PEI ( $\Phi = 0.5\%$ ). For higher  $\Phi = 1\%$ , the Ia3d phase is transformed into the reverse hexagonal phase,  $H_{II}$ . On increasing  $\Phi$  to 2%, the GMO/water/2kDa PEI system forms the Fd3m phase. Similarly, for higher water content  $30\% < f_w \leq 40\%$ , the double diamond Pn3m phase forms (characterized by SAXS peaks, whose positions are in the ratio of  $\sqrt{2} : \sqrt{3} : \sqrt{4}$ ). For ternary systems at these  $f_w$  too, we observe the formation of a reverse hexagonal  $H_{II}$  phase for  $\Phi = 1\%$  and of the Fd3m phase for  $2\% \leq \Phi \leq 4\%$ . Thus, while GMO/water systems form  $L_\alpha$ , Ia3d and Pn3m phases with increasing  $f_w$  between 10-40%, at all these  $f_w$ , they organize to form an  $H_{II}$  phase at intermediate  $\Phi$  and transform into an Fd3m phase at higher  $\Phi$ .

#### b. GMO/water/PEI-2kDa: Effect of temperature:

On heating, the GMO/water binary system transforms into an isotropic reverse micellar phase ( $L_2$ ) at all  $10\% \leq f_w \leq 40\%$ . For low  $f_w = 10\%$ , GMO/water directly transforms from the  $L_\alpha$  to the  $L_2$  phase above  $\approx 40^\circ\text{C}$  (Figure 4). For  $10\% < f_w \leq 20\%$ , the  $L_\alpha$  phase transforms into the cubic Ia3d (above  $25^\circ\text{C}$ ) and finally to the  $L_2$  phase (between  $45$ - $60^\circ\text{C}$ ). At higher  $f_w < 35\%$ , there is a transition from the Ia3d to the Pn3m phase on heating to  $30$ - $50^\circ\text{C}$ , and then into the  $H_{II}$  phase and finally into the  $L_2$  phase ( $> 65^\circ\text{C}$ ). Finally, for  $f_w > 35\%$ , the cubic Pn3m phase transforms into the  $H_{II}$  phase (at  $\approx 60^\circ\text{C}$ ) and finally to the  $L_2$  phase (between  $70$ - $75^\circ\text{C}$ ). The temperature dependence of the lipid phase behaviour can be rationalized using packing parameter arguments. With increase in temperature,

there is a larger entropic free energy penalty for water molecules associated with the head group.<sup>53</sup> Therefore, an increase in temperature results in a concomitant increase in P that corresponds to a transition from  $L_\alpha$  through cubic, hexagonal and, inverse micellar phases.

For  $f_w = 10\%$ , addition of PEI ( $0.5\% \leq \Phi \leq 4\%$ ) induces the formation of the  $H_{II}$  phase at  $25^\circ\text{C}$ , that transforms into the  $L_2$  phase between  $60$ - $80^\circ\text{C}$ . For  $f_w = 15$ - $40\%$  and, for  $\Phi = 1\%$ , the  $H_{II}$  phase forms at room temperature and transforms into the  $L_2$  phase between  $50$ - $75^\circ\text{C}$  (Figure 4). For  $f_w = 15$ - $40\%$  and,  $2\% \leq \Phi \leq 4\%$ , the Fd3m phase forms at  $25^\circ\text{C}$  and transforms on heating into the  $L_2$  phase (between  $40$ - $65^\circ\text{C}$ , Figure 4). The Fd3m/ $L_2$  transition happens at higher temperature ( $\approx 65^\circ\text{C}$ ) for  $\Phi = 2\%$  and, decreases to  $\approx 40^\circ\text{C}$  with increase in  $\Phi$ . Thus, in general, we observe that in ternary compositions containing PEI, transition temperatures to higher curvature states are suppressed relative to the binary GMO/water system. The higher the PEI concentration ( $\Phi$ ) in the ternary system, the lower is the transition temperature to the  $L_2$  phase. Again, we note that the high curvature reverse micellar Fd3m phase is not accessible for the binary GMO/water system. Addition of PEI ( $\Phi \geq 2\%$ ) to GMO/water affords the formation of reverse micellar phases at sufficiently low temperatures, where the micelles can crystallize into an  $AB_2$  cubic structure (the Fd3m phase). On heating, the cubic ordering of the micelles cannot be sustained and the Fd3m phase transitions to an isotropic reverse micellar phase.

#### c. Influence of PEI molecular weight:

Finally, we investigate the influence of PEI molecular weight on the phase behaviour of GMO/water/PEI. We present data for ternary systems containing PEI with molecular weights,  $M_w$

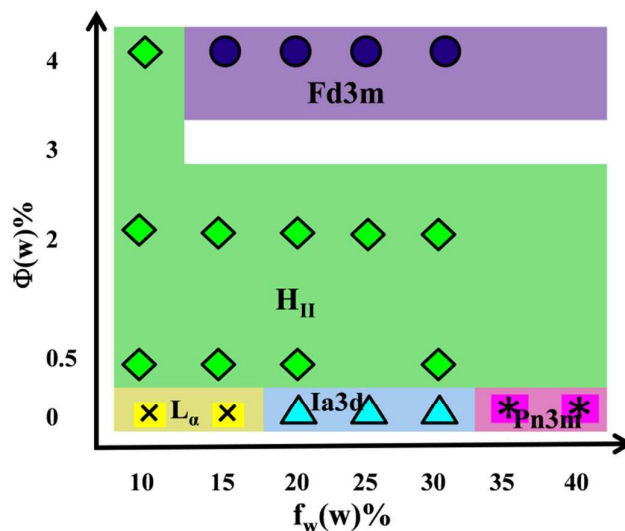
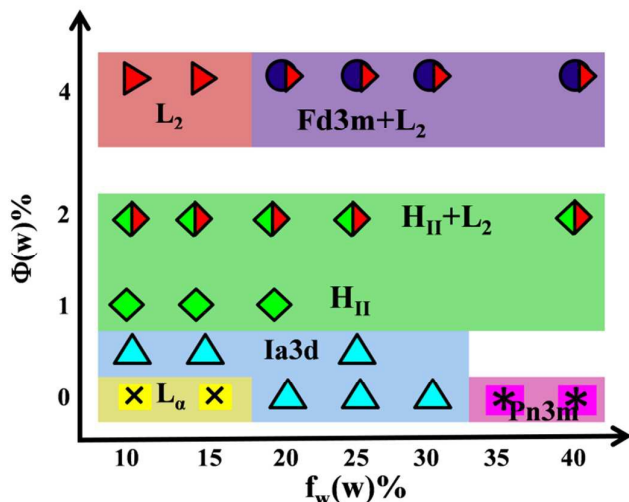


Figure 5: Phase behaviour of the ternary system GMO/water/0.8 kDa PEI at  $T = 25^\circ\text{C}$ .

= 0.8 kDa and 25 kDa and, contrast with data on systems containing 2 kDa PEI. Ternary systems containing 0.8 kDa PEI show similar behaviour as those containing 2kDa PEI, at

matched  $\Phi$  (Figure 5). For  $f_w \leq 15\%$ , GMO/water transitions from an  $L_\alpha$  phase at  $\Phi = 0\%$  to an  $H_{II}$  phase at  $\Phi = 0.5\%$ . We do not observe an intermediate cubic phase for the ternary system containing 0.8 kDa PEI. Similar to the case of 2 kDa PEI, the  $f_w = 10\%$  system stays in the  $H_{II}$  phase up to  $\Phi = 4\%$ . At  $f_w = 15\%$  the  $H_{II}$  phase transforms into the Fd3m for  $\Phi$  between 2-4%. For  $20\% \leq f_w \leq 30\%$ , the Ia3d phase transforms into the  $H_{II}$  phase up for  $\Phi = 0.5\%$ , and into the Fd3m phase at  $\Phi$  between 2-4%. Thus, the  $H_{II}$ /Fd3m phase transition happens only for higher PEI loadings for the lower molecular weight polymer.



**Figure 6:** Phase behaviour of the ternary system GMO/water/25 kDa PEI at  $T = 25^\circ\text{C}$ .

For systems containing the high molecular weight polymer (25 kDa PEI), the formation of the reverse micellar Fd3m phase is significantly inhibited (Figure 6). SAXS peaks corresponding to the Fd3m phase are observed only for samples with  $f_w \geq 20\%$  and  $\Phi = 4\%$  however, here the Fd3m phase coexists with the isotropic  $L_2$  phase.  $L_2$ / $H_{II}$  phase coexistence is observed at room temperature for  $10\% \leq f_w \leq 40\%$  at  $\Phi = 2\%$ , unlike systems containing 2 kDa PEI, where the  $L_2$  phase is never observed at  $25^\circ\text{C}$ . For ternary systems containing 25 kDa PEI, increasing  $\Phi$  leads to a transition from  $L_\alpha$  to cubic Ia3d ( $\Phi = 0.5\%$ ) to  $H_{II}$  ( $\Phi = 1\%$ ) to  $H_{II}/L_2$  ( $\Phi = 2\%$ ) and finally  $L_2$  ( $\Phi = 4\%$ ) for low water content ( $f_w \leq 15\%$ ) compositions. For higher water content ( $f_w \geq 20\%$ ), the cubic phases formed at  $\Phi = 0\%$  transition into an  $H_{II}$  phase at  $\Phi = 1\%$ ;  $H_{II}/L_2$  coexistence at  $\Phi = 2\%$  and Fd3m/ $L_2$  coexistence at  $\Phi = 4\%$  (Figure 6).

Thus, our data suggests that addition of 2kDa PEI is most efficacious in inducing the formation of the Fd3m phase. Our previous investigations suggest that formation of the Fd3m phase happens due to strong attractive interactions between the lipid headgroup and PEI amines.<sup>48</sup> The compact shape of the branched PEI is essential for inducing Fd3m phase formation. Analogous linear molecules bearing amine groups do not induce Fd3m formation in GMO/water systems.<sup>48</sup> Following our previous work,<sup>48</sup> we believe that topologically compact molecules, such as the branched PEI, are unable to

extend on the GMO surface to maximize headgroup-amine interactions. Therefore, GMO engulfs the PEI molecules to create high curvature assemblies.

The Fd3m phase comprises micelles of two different sizes packed into an  $AB_2$  structure. While other single component lipids have been shown<sup>54</sup> to organize to form such bidisperse micellar assemblies, neat GMO/water systems are not known to form an Fd3m phase. In the present study, it is possible that localization of the PEI molecules within micellar GMO structures is responsible for the formation of the Fd3m phase. The Fd3m phase forms when the two micelles in the  $AB_2$  structure have a size ratio of  $0.482 \leq B/A \leq 0.624$ .<sup>55</sup> Our data suggests that the 2 kDa PEI has the right molecular size to facilitate formation of the Fd3m phase. The high molecular weight 25 kDa PEI has a molecular size that is significantly larger than the 2 kDa polymers. Accordingly, we observe a stronger tendency to form the less ordered isotropic  $L_2$  phase. We also note that the 25 kDa PEI has a higher polydispersity index relative to the 0.8 and 2 kDa PEI. Therefore, the formation of the  $H_{II}$  and Fd3m phases that coexist with the  $L_2$  phase for ternary systems comprising 25 kDa PEI might be a consequence of the PEI polydispersity. Sorting of added polymer chains by their molecular weight ("sieving") by surfactant mesophases has been reported in the literature.<sup>18</sup> It is possible that the low molecular mass components of the polydisperse 25 kDa PEI are responsible for formation of the  $H_{II}$  and Fd3m phases in GMO/water, that coexist with the disordered  $L_2$  phase.

The equilibrium structure formed when PEI is incorporated in GMO/water is governed by several factors. Firstly, PEI interacts with GMO and, dehydrates the head group size resulting in a change in the effective head group size. The conformational entropy of the PEI is reduced when it is incorporated within the organized lipid structure. This change in conformational entropy is a function of polymer architecture: chain molecular weight and branched structure. Our results indicate that this combination of factors results in an enhanced stability window for the Fd3m phase for a PEI molecular weight of 2 kDa.

## Summary

We present a detailed investigation of the phase behaviour of ternary glycerol monooleate/water/PEI systems. GMO/water systems containing small fractions ( $\Phi = 2\text{-}4\%$ ) of low molecular weight PEI ( $M_w = 0.8$  kDa, 2 kDa) form an ordered reverse micellar cubic phase with Fd3m symmetry. For higher molecular, relatively polydisperse PEI ( $M_w = 25$  kDa), the Fd3m phase forms at  $\Phi = 4\%$  PEI, in coexistence with the isotropic  $L_2$  phase. For all compositions, we observe an Fd3m/ $L_2$  phase transition on heating to sufficiently high temperatures. The formation of the discontinuous reverse micellar Fd3m phase at room temperature has implications for systems for controlled delivery of water soluble actives. Diffusion of encapsulated actives through a discontinuous phase (such as the Fd3m) has been demonstrated<sup>56,57</sup> to be dramatically slower as compared to through bicontinuous cubic phases, suggesting the use of Fd3m cubosomes for slow release formulations. Further, our

investigation reveals that the temperature window for stability of the Fd3m phase is a strong function of the PEI molecular weight. This work provides guidelines for the design of polymer chain architecture (viz. branching, molecular weight and exposed functional groups) of ternary inclusions for optimal design of temperature stable, slow release formulations.

## Acknowledgements

GK acknowledges funding from DST Chemical Engineering PAC through project DST/SR/S3/CE/029/2011. We also gratefully acknowledge support from the CSIR Five Year Plan programme, M2D (CSC-0134). MK acknowledges a research fellowship from UGC. We thank Gaurav Chaudhry from Danisco for supplying us Rylo.

## Notes and references

- D. P. Siegel, *Biophys. J.*, 1999, **76**, 291-313.
- C. Fong, T. Le and C. J. Drummond, *Chem. Soc. Rev.*, 2012, **41**, 1297-1322.
- A. Angelova, B. Angelov, V. M. Garamus, P. Couvreur and S. Lesieur, *J. Phys. Chem. Lett.*, 2012, **3**, 445-457.
- R. Mezzenga, P. Schurtenberger, A. Burbidge and M. Michel, *Nat. Mater.*, 2005, **4**, 729-740.
- M. Caffrey, *J. Struct. Biol.*, 2003, **142**, 108-132.
- C. Ostermeier and H. Michel, *Curr. Opin. Struct. Biol.*, 1997, **7**, 697-701.
- S. Mann and G. A. Ozin, *Nature*, 1996, **382**, 313-318.
- C. V. Kulkarni, W. Wachter, G. Iglesias-Salto, S. Engelskirchen and S. Ahualli, *Phys. Chem. Chem. Phys.*, 2011, **13**, 3004-3021.
- A. Ganem-Quintanar, D. Quintanar-Guerrero and P. Buri, *Drug Dev. Ind. Pharm.*, 2000, **26**, 809-820.
- C. J. Drummond and C. Fong, *Curr. Opin. Colloid Interface Sci.*, 1999, **4**, 449-456.
- S. Deshpande, E. Venugopal, S. Ramagiri, J. R. Bellare, G. Kumaraswamy, N. Singh, *ACS App. Mater. Interfaces* 2014, **6**, 17126-17133.
- T. Landh, *J. Phys. Chem.*, 1994, **98**, 8453-8467.
- J. Barauskas, M. Johnsson and F. Tiberg, *Nano Lett.*, 2005, **5**, 1615-1619.
- P. T. Spicer, *Curr. Opin. Colloid Interface Sci.*, 2005, **10**, 274-279.
- C. V. Kulkarni, R. Mezzenga and O. Glatter, *Soft Matter*, 2010, **6**, 5615-5624.
- G. Kumaraswamy and K. P. Sharma, *Advances in Planar Lipid Bilayers and Liposomes*, 2013, **18**, 181.
- M. N. Wadekar, R. Pasricha, A. B. Gaikwad and G. Kumaraswamy, *Chem. Mater.*, 2005, **17**, 2460-2465.
- I. E. Pacios, C. S. Renamayo, A. Horta, K. Thuresson and B. r. Lindman, *Macromolecules*, 2005, **38**, 1949-1957
- C. A. Guymon, E. N. Hoggan, N. A. Clark, T. P. Rieker, D. M. Walba and C. N. Bowman, *Science*, 1997, **275**, 57-59.
- H. E. Warriner, S. H. J. Idziak, N. L. Slack, P. Davidson and C. R. Safinya, *Science*, 1996, **271**, 969-973.
- R. Mezzenga, M. Grigorov, Z. Zhang, C. Servais, L. Sagalowicz, A. I. Romoscanu, V. Khanna and C. Meyer, *Langmuir*, 2005, **21**, 6165-6169.
- A. Yaghmur, P. Laggner, S. Zhang and M. Rappolt, *PLoS One*, 2007, **2**, 479.
- A. Bilalov, J. Elsing, E. Haas, C. Schmidt and U. Olsson, *J. Colloid Interface Sci.*, 2013, **394**, 360-367.
- J. O. Radler, I. Koltover, T. Salditt and C. R. Safinya, *Science* 1997, **275**, 810-814.
- B. Ericsson, K. Larsson and K. Fontell, *BBA-Biomembranes*, 1983, **729**, 23-27.
- K. Larsson, *J. Phys. Chem.*, 1989, **93**, 7304-7314.
- S. Tanaka, S. Maki and M. Ataka, *Phys. Rev. E*, 2006, **73**, 061510.
- S. Guillot, S. Salentinig, A. Chemelli, L. Sagalowicz, M. E. Leser and O. Glatter, *Langmuir*, 2010, **26**, 6222-6229.
- B. Angelov, A. Angelova, B. Papahadjopoulos-Sternberg, S. Lesieur, J. F. Sadoc, M. Ollivon and P. Couvreur, *J. Am. Chem. Soc.*, 2006, **128**, 5813-5817.
- C. Leal, K. K. Ewert, N. F. Boussein, R. S. Shirazi, Y. Li and C. R. Safinya, *Soft Matter*, 2013, **9**, 795-804.
- A. Angelova, B. Angelov, R. Mutafchieva, S. Lesieur, P. Couvreur, *Acc. Chem. Res.*, 2010, **44**, 147-156.
- J. N. Israelachvili, *Intermolecular and Surface Forces*, Academic press London, San Diego, 2nd edn, 1991.
- X. Mulet, R. H. Templer, R. Woscholski and O. Ces, *Langmuir*, 2008, **24**, 8443-8447.
- Y. Misquitta and M. Caffrey, *Biophys. J.*, 2003, **85**, 3084-3096.
- V. Cherezov, J. Clogston, M. Z. Papiz and M. Caffrey, *J. Mol. Biol.*, 2006, **357**, 1605-1618.
- Z. Wang, L. Zheng and T. Inoue, *J. Colloid Interface Sci.*, 2005, **288**, 638-641.
- I. Amar-Yuli, E. Wachtel, E. B. Shoshan, D. Danino, A. Aserin and N. Garti, *Langmuir*, 2007, **23**, 3637-3645.
- A. Yaghmur, L. de Campo, S. Salentinig, L. Sagalowicz, M. E. Leser and O. Glatter, *Langmuir*, 2005, **22**, 517-521.
- A. Yaghmur, L. de Campo, L. Sagalowicz, M. E. Leser and O. Glatter, *Langmuir*, 2005, **21**, 569-577.
- M. Pouzot, R. Mezzenga, M. Leser, L. Sagalowicz, S. Guillot and O. Glatter, *Langmuir*, 2007, **23**, 9618-9628.
- S. Phan, W. K. Fong, N. Kirby, T. Hanley and B. J. Boyd, *Int. J. Pharm.*, 2011, **421**, 176-182.
- L. Sagalowicz, S. Guillot, S. Acquistapace, B. Schmitt, M. Maurer, A. Yaghmur, L. de Campo, M. Rouvet, M. Leser and O. Glatter, *Langmuir*, 2013, **29**, 8222-8232.
- I. Martiel, L. Sagalowicz and R. Mezzenga, *Adv. Colloid Interface Sci.*, 2014, **209**, 127-143.
- I. Martiel, L. Sagalowicz and R. Mezzenga, *Langmuir*, 2014, **29**, 15805-15812.
- G. C. Shearman, A. I. I. Tyler, N. J. Brooks, R. H. Templer, O. Ces, R. V. Law and J. M. Seddon, *Liq. Cryst.*, 2010, **37**, 679-694.
- J. M. Seddon, J. Robins, T. Gulik-Krzywicki and H. Delacroix, *Phys. Chem. Chem. Phys.*, 2000, **2**, 4485-4493
- P. M. Duesing, R. H. Templer and J. M. Seddon, *Langmuir*, 1997, **13**, 351-359.
- M. Kumar, N. G. Patil, C. K. Choudhury, S. Roy, A. V. Ambade and G. Kumaraswamy, *Soft Matter*, 2015, DOI: 10.1039/C5SM00854A
- C. K. Choudhury, A. Kumar and S. Roy, *Biomacromolecules*, 2013, **14**, 3759-3768.
- C. K. Choudhury and S. Roy, *Soft Matter*, 2013, **9**, 2269-2281.
- K. P. Sharma, C. K. Choudhury, S. Srivastava, H. Davis, P. R. Rajamohanam, S. Roy and G. Kumaraswamy, *J. Phys. Chem. B*, 2011, **115**, 9059-9069.
- V. Luzzati, R. Vargas, A. Gulik, P. Mariani, J. M. Seddon and E. Rivas, *J. Biochem.*, 1992, **31**, 279-285.
- W. B. Lee, R. Mezzenga and G. H. Fredrickson, *Phys. Rev. Lett.*, 2007, **99**, 187801
- J. M. Seddon, N. Zeb, R. H. Templer, R. N. McElhane and D. A. Mannock, *Langmuir*, 1996, **12**, 5250-5253.
- M. J. Murray and J. V. Sanders, *Philosophical Magazine A*, 1980, **42**, 721-740.
- S. Phan, W. K. Fong, N. Kirby, T. Hanley and B. J. Boyd, *Int. J. Pharm.*, 2011, **421**(1), 176-182



## ARTICLE

Journal Name

57 I. Martiel, N. Baumann, J. J. Vallooran, J. Bergfreund, L. Sagalowicz and R. Mezzenga, *J. Control. Release*, 2015, **204**, 78-84.

Soft Matter Accepted Manuscript